Efficiency and finite size effects in enhanced transmission through subwavelength apertures

F. Przybilla[1], A. Degiron[1], C. Genet[1], T. W. Ebbesen[1],
F. de Léon-Pérez[2], J. Bravo-Abad[3], F. J. García-Vidal[3],
L. Martín-Moreno[2]

[1]*Laboratoire des Nanostructures, ISIS, Université Louis Pasteur and CNRS (UMR7006),*
8 allée Gaspard Monge, F-67000 Strasbourg, France
ebbesen@isis-ulp.org

[2]*Departamento de Física de la Materia Condensada-ICMA, Universidad de Zaragoza-CSIC,*
E-50009 Zaragoza, Spain

[3]*Departamento de Física Teórica de la Materia Condensada, Universidad Autónoma de*
Madrid, E-28049 Madrid, Spain

Abstract: We investigate transmission efficiency and finite size effects for the subwavelength hole arrays. Experiments and simulations show how the finite size effects depend strongly on the hole diameter. The transmission efficiency reaches an asymptotic upper value when the array is larger than the surface plasmon propagation length on the corrugated surface. By comparing the transmission of arrays with that of the corresponding single holes, the relative enhancement is found to increase as the hole diameter decreases. In the conditions of the experiments the enhancement is one to two orders of magnitude but there is no fundamental upper limit to this value.

OCIS codes: (050.1220) Apertures; (240.6680) Surface plasmons; (050.2770) Gratings; (050.1960) Diffraction theory; (050.6624) Subwavelength structures.

References and links

1. T. W. Ebbesen, H. J. Lezec, H. F. Ghaemi, T. Thio, and P. A. Wolff, "Extraordinary optical transmission through sub-wavelength hole arrays," Nature **391,** 667 (1998).
2. L. Martín-Moreno, F. J. García-Vidal, H. J. Lezec, K. M. Pellerin, T. Thio, J. B. Pendry, and T. W. Ebbesen, "Theory of extraordinary optical transmission through subwavelength hole arrays," Phys. Rev. Lett. **86,** 1114 (2001).
3. C. Genet and T. W. Ebbesen, "Light in tiny holes," Nature **445,** 39 (2007).
4. R. Wannemacher, "Plasmon-supported transmission of light through nanometric holes in metallic thin films," Opt. Commun. **195,** 107 (2001).
5. A. Degiron, H. J. Lezec, N. Yamamoto, and T. W. Ebbesen, "Optical transmission properties of a single sub-wavelength aperture in a real metal," Opt. Commun. **239,** 61 (2004).
6. K. L. van der Molen, K. J. Klein Koerkamp, S. Enoch, F. B. Segerink, N. F. van Hulst, and L. Kuipers, "Role of shape and localized resonances in extraordinary transmission through periodic arrays of subwavelength holes: experiment and theory," Phys. Rev. B **72,** 045421 (2005).
7. F. J. García de Abajo, "Light transmission through a single cylindrical hole in a metallic film," Opt. Express **10,** 1475 (2002).
8. F. J. García-Vidal, E. Moreno, J. A. Porto and L. Martín-Moreno, "Transmission of light through a single rectangular hole," Phys. Rev. Lett. **95,** 103901 (2005).

9. E. Popov, N. Bonod, M. Nevière, H. Rigneault, P.-F. Lenne and P. Chaumet, "Surface plasmon excitation on a single subwavelength hole in a metallic sheet," Appl. Opt. **44,** 2332 (2005).

10. F. J. García-Vidal, L. Martín-Moreno, Esteban Moreno, L. K. Kumar, and R. Gordon, "Transmission of light through a single rectangular hole in a real metal," Phys. Rev. B **74,** 153411 (2006).

11. T. Rindzevicius, Y. Alaverdyan, B. Sepulveda, T. Pakizeh, M. Käll, R. Hillenbrand, J. Aizpurua and F. J. García de Abajo, "Nanohole plasmons in optically thin gold films," J. Phys. Chem. C **111,** 1207 (2007).

12. A. Degiron and T. W. Ebbesen, "The role of localized surface plasmon modes in the enhanced transmission of periodic subwavelength apertures," J. Opt. A: Pure Appl. Opt. **7,** S90 (2005).

13. J. Bravo-Abad, F. J. García-Vidal and L. Martín-Moreno, "Resonant transmission of light through finite chains of subwavelength holes in a metallic film," Phys. Rev. Lett. **93,** 227401 (2004).

14. T. Thio, H. F. Ghaemi, H. J. Lezec, P. A. Wolff and T. W. Ebbesen, "Surface-plasmon-enhanced transmission through hole arrays in Cr films," J. Opt. Soc. Am. B **16,** 1743 (1999).

15. F. Miyamaru and M. Hangyo, "Finite size effect of transmission property for metal hole arrays in subterahertz region," Appl. Phys. Lett. **84,** 2742 (2004).

16. J. Henzie, M. H. Lee and T. W. Odom, "Multiscale patterning of plasmonic metamaterials," Nat. Nanotechnol. **2,** 549 (2007).

17. J. Bravo-Abad, A. Degiron, F. Przybilla, C. Genet, F. J. García-Vidal, L. Martín-Moreno and T. W. Ebbesen, "How light emerges from an illuminated array of subwavelength holes," Nat. Phys. **2,** 120 (2006).

18. A. Krishnan, T. Thio, T. J. Kim, H. J. Lezec, T. W. Ebbesen, P. A. Wolff, J. Pendry, L. Martín-Moreno and F. J. García-Vidal, "Evanescently coupled resonance in surface plasmon enhanced transmission," Opt. Commun. **200,** 1 (2001).

19. M. Sarrazin, J.-P. Vigneron and J.-M. Vigoureux, "Role of Wood anomalies in optical properties of thin metallic films with a bidimensional array of subwavelength holes," Phys. Rev. B **67,** 085415 (2003).

20. C. Genet, M. P. van Exter and J. P. Woerdman, "Fano-type interpretation of red shifts and red tails in hole array transmission spectra," Opt. Commun. **225,** 331 (2003).

21. S. G. Rodrigo, F. J. García-Vidal and L. Martín-Moreno, "Influence of material properties on extraordinary optical transmission through hole arrays," Phys. Rev. B **77,** 075401 (2008).

22. E.D. Palik, *Handbook of Optical Constants of Solids* (London, Academic 1985)

23. A. Vial, A.-S. Grimault, D. Macias, D. Barchiesi, and M.L. de la Chapelle, " Improved analytical fit of gold dispersion: Application to the modeling of extinction spectra with a finite-difference time-domain method," Phys. Rev. B **71**, 085416 (2005).

24. D. S. Kim, S. C. Hohng, V. Malyarchuk, Y. C. Yoon, Y. H. Ahn, K.J. Yee, J.W. Park, J. Kim, Q.H. Park and C. Lienau, "Microscopic origin of surface-plasmon radiation in plasmonic band-gap nanostructures," Phys. Rev. Lett. **91,** 143901 (2003).

25. C. Obermüller, and K. Karrai, "Far field characterisation of diffracting circular apertures," Appl. Phys. Lett. **67,** 3408 (1995).

26. E. Popov, M. Nevière, A. Sentenac, N. Bonod, A. L. Fehrembach, J. Wenger, P.-F. Lenne and H. Rigneault, "Single-scattering theory of light diffraction by a circular subwavelength aperture in a finitely conducting screen," J. Opt. Soc. Am. A **24,** 339 (2007).

27. C. Obermüller, K. Karrai, G. Kolb and G. Abstreiter, "Transmitted radiation through a subwavelength-sized tapered optical fiber tip," Ultramicroscopy **61,** 171 (1995).

28. K. L. van der Molen, F. B. Segerink, N. F. van Hulst, and L. Kuipers, "Influence of hole size on the extraordinary transmission through subwavelength hole arrays," Appl. Phys. Lett. **85,** 4316 (2004).

29. H. Shin, P. B. Catrysse, and S. Fan, "Effect of the plasmonic dispersion relation on the transmission properties of subwavelength cylindrical holes," Phys. Rev. B **72,** 085436 (2005).

30. F. Przybilla, A. Degiron, J.-Y. Laluet, C. Genet and T. W. Ebbesen, "Optical transmission in perforated noble and transition metal films," J. Opt. A: Appl. Opt. **8,** 458 (2006).

31. H. A. Bethe, "Theory of diffraction by small holes," Phys. Rev. **66,** 163 (1944).

1. Introduction

It is now well established that an array of subwavelength apertures in an opaque metal film can give rise to a transmission much larger than the sum of the transmissions of the individual holes taken separately. The transmission enhancement relies on the resonant excitation of surface plasmons (SPs) by the incident light. This interaction is made possible by the additional momentum (grating momentum) provided by the scattering of the incident light by the hole array [1, 2, 3]. In addition, excitation of localized surface plasmons [4-6] and other modes [7-11] may also play a role in the process although the grating momentum appears to define the main resonances of the transmission spectrum [3, 12, 13], specially in the case of arrays of circular

holes. As the number of period increases, the structure factor peaks appearing at reciprocal lattice vectors get better defined, the size of the structure is therefore expected to influence the coupling of light with SPs. Indeed, experimental measurements in the infrared [14], in the THz wave region [15] and in the visible [16] confirm this expectation. In addition, finite size also affects the re-emission pattern from the array [17].

Since arrays of apertures are always finite, it is important to understand in detail all the consequences of the actual size for both fundamental reasons and when considering the numerous applications of such structures [3]. In the following, we report both experimental and theoretical work on finite size effects in 2D arrays of subwavelength holes in the visible, focusing on the spectral response of arrays, the role of the SP propagation length and its connection to the maximum enhancement factor that can be achieved for the transmission.

2. Finite size effects in the enhanced transmission phenomenon

For the first part of this study, we fabricated finite square arrays of sub-wavelength holes of different sizes. The structures milled through a $275nm$ freestanding Ag film using focused ion beam (FIB, Ga ions), consist of holes arranged in a square lattice of period $P = 600nm$. The advantage of a freestanding metal film is that the dielectric constant is the same on both sides of the film, a configuration that optimizes transmission efficiencies [18]. An optical microscope coupled to a spectrometer was used to measure the transmission spectra of the samples that were illuminated by a collimated incident beam at normal incidence. The transmitted light is collected with a $40\times$ objective (with 0.6 numerical aperture).

We recall that the transmission spectra of such arrays are characterized by resonances (peaks in the transmission spectra) which are related to a (i,j) scattering order of the array. The wavelength of these resonances are given in a first approximation [1], by:

$$\lambda_{(i,j)} = \frac{P}{\sqrt{i^2 + j^2}} \sqrt{\frac{\varepsilon_m \varepsilon_d}{\varepsilon_m + \varepsilon_d}} \qquad (1)$$

where ε_m and ε_d are respectively the dielectric constants of the metal and the dielectric (in this case air), and P the period of the array. The actual peaks are red-shifted compared to the predictions of Eq. (1) since it doesn't take into account the presence of holes and scattering losses. Nevertheless it provides a simple means to label and associate the various peaks with the corresponding (i,j) scattering order.

At first we measured the transmission spectra of arrays with increasing number of holes (N) with constant diameter $d = 268nm$ as shown in Fig. 1(a). The peaks can be labelled by (i,j) according to the predictions of Eq. (1). Let us focus on the $(1,0)$ peak at around $680nm$ which is spectrally isolated. The maximum transmission increases with N, and eventually exceeds unity as normalized to the hole area. In this regime, the photon flux emerging from a given aperture is larger than the flux incident on this aperture. This corresponds to the extraordinary optical transmission (EOT) regime [1]. With the particular parameters of this sample, this special condition is already fulfilled for the 21×21 hole array. It should be also noted that the resonance peak profile becomes asymmetric with a blue shift as N increases. This is consistent with an increase in the SP resonant contribution with respect to that of the direct transmission through the holes. Consequently as the SP mode becomes spectrally better defined with N, it takes on the typical asymmetrical shape expected from the Fano analysis [19, 20].

The calculation of the transmission spectra in infinite periodic arrays can nowadays be done with arbitrary precision, for instance by using the finite difference time domain method (FDTD) [21]. This method compares very well with experiments in the limit of very large arrays. Smaller arrays, however, can only be approximately treated. In this work, calculations have been carried out using a theoretical framework based on a modal expansion (ME) of the electromagnetic
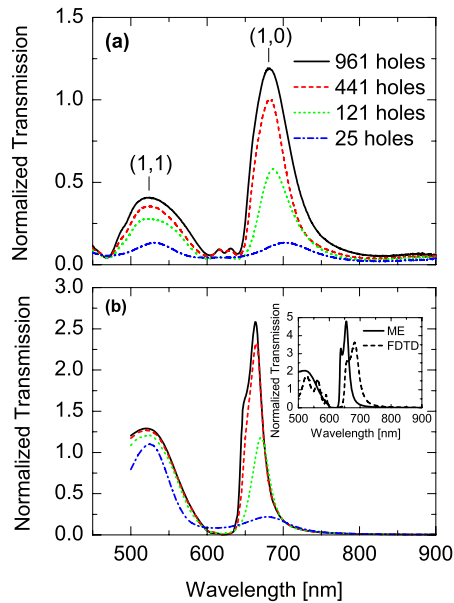
Fig. 1. (Color online) (a) Experimental transmission spectra for finite size arrays made of 5×5, 11×11, 21×21 and 31×31 holes. The arrays were milled in thick $275nm$ suspended Ag film with a period $P = 600nm$ and a hole diameter $d = 268nm$. Transmissions are normalized to the hole area. The ticks indicate the position of main resonances labelled according the index (i, j) presented in Eq. (1). (b) Transmission spectra, normalized also to the area occupied by the holes, obtained from the numerical simulations using the modal expansion (ME) formalism. The geometrical parameters are the same as in the experiments. Inset: Comparison of ME and finite difference time domain (FDTD) calculations for the infinite array.

fields in the different regions of the structure. Details of this numerical technique, which is ideally suited to treat finite collections of indentations drilled on a metallic film, can be found in Ref. [13]. Let us briefly sketch here the basic approximations used in order to treat real metals. In a first step, the metal is approximated by a perfect conductor. Then, surface impedance boundary conditions (SIBCs) are applied to the horizontal interfaces of the film in order to take into account the finite dielectric constant of the metal at optical frequencies. For both Ag and Au, the dielectric constants were fitted from tabulated optical data [22], using the Drude-Lorentz model and the procedure reported in [23]. When considering the propagation constant of the fundamental mode inside the hole waveguide, we take its value from an independent calculation done for a circular hole perforated on a real metal (in this case, Ag). Additionally, in order to consider the penetration of the electromagnetic fields inside the metal, the diameter of the holes is (phenomenologically) enlarged by two times the skin depth of the metal [2]. In order to estimate the validity of the ME approach, inset of Fig. 1(b) shows the comparison between FDTD transmission spectra (computed for a mesh size of $5nm$) and the ME ones for an infinite periodic array. The ME results nicely reproduce the existence of EOT peaks. However, for these geometrical parameters, which are typical in EOT experiments, the ME predicts transmission peaks that are blueshifted by about $25nm$ from FDTD. Also, while the integrated resonant transmission computed within the ME is very close to the "exact" value predicted by FDTD, approximated peaks are about 40% higher and about 40% narrower. These are values to keep in mind when comparing with experiments since they indicate that the ME results will have only

semiquantitative value. Nevertheless, as the comparison with experimental data in this work will show, trends in the dependences on the different geometrical parameters are well captured by the ME approximation. Figure 1(b) renders the computed results of the transmission spectra of arrays with the same geometrical parameters as in the experiments. The observed evolution of the experimental transmission spectrum as the number of holes is increased is well reproduced in our theoretical calculations.
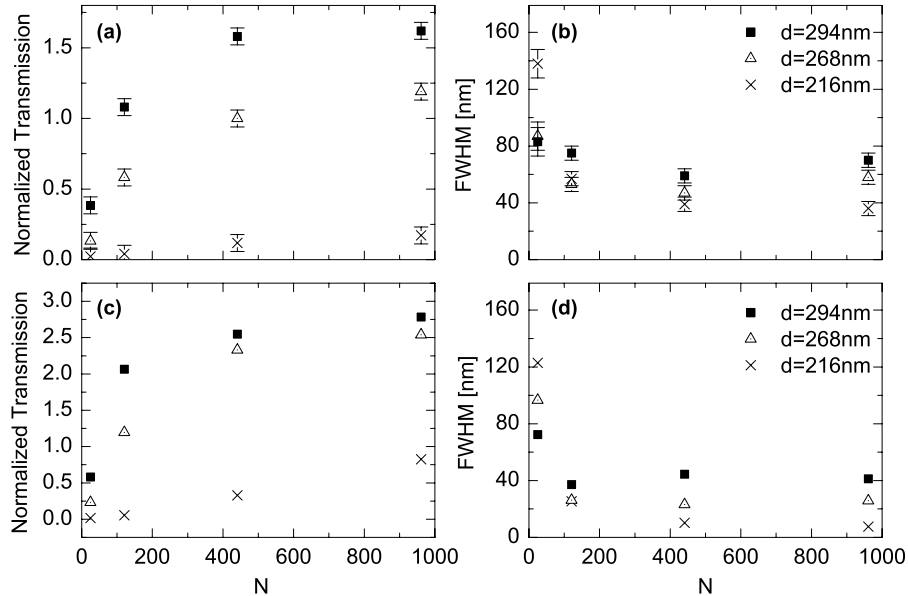

Fig. 2. (a) Experimental normalized maximum transmitted intensities as a function of the number of holes (N) for increasing hole diameters (d = 216, 268 and 294nm). (b) Experimental full width at half maximum (FWHM) corresponding to the data presented in panel (a). (c) and (d) Results of the numerical simulations using the same geometrical parameters as in the experiments presented in panel (a) and (b). Errors bars are determined from the data dispersions obtained from several measurements on separate structures on a test sample.

In order to have more insights into the phenomenon, we repeated the experiment for different hole diameters. The measurements, presented in Fig. 2(a), follow the same tendency as described previously, i.e., maximum transmitted intensity rises as N increases. However as can be seen, the larger the hole diameter, the faster a transmission saturation is reached. As seen on Fig. 2(c), theoretical calculations based on ME clearly capture experimental trends, with however slight differences in intensities. As stressed above, ME calculations always predict higher transmissions and smaller FWHMs than FDTD simulations. This amounts to a systematic difference in the theory that is sufficient to explain the discrepancies between experiments and ME simulations, as seen when comparing Figs. 2(a) and (c). Nevertheless both simulations and experimental capture the fact that the transmission increases with the size of the array and reaches a saturation. The rate at which the transmission reaches saturation increases with d.

To reveal the underlying mechanism it is interesting to follow the full widths at half maximum (FWHM) of the resonances, which is a measure of the lifetime of the SPs on the array [2, 24]. As shown in Fig. 2(b), for all the diameters considered, FWHM decreases towards horizontal asymptotes as N is increased. These lower limits correspond to the total losses of the systems, i.e. internal (absorption inside the metal) and radiative losses (largest contribution).
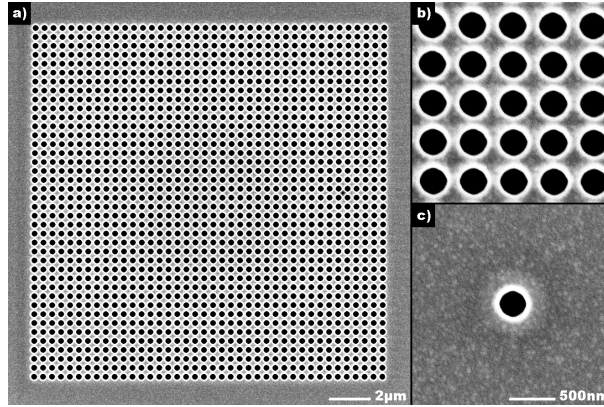
Fig. 3. (a) and (b) Scanning electron microscopy images of an array of 40×40 holes ($P = 430nm$ and $d = 300nm$) milled through a $295nm$ thick Au film. (c) Corresponding single hole. Images presented in panels (b) and (c) have the same scale. As it can be seen in panels (b) and (c), geometrical parameters of the holes are as identical as possible at the level of the array or at the single hole level.

As can be seen in our experiments, the value of these asymptotes increase with the hole diameter. Given the fact that all the structures where milled in the same film with the same level of precision, this tendency can be explained by the fact that increasing the hole diameter increases the scattering undergone by the SPs over the array and, therefore, increases the radiative losses and the value of the asymptotes [24]. Considering these asymptotic values and assuming an exponential decay of the SPs, it is possible to evaluate the maximum propagation length of SP ($l_{SP_{max}}$) for an infinite array. We obtain values of $\sim 2.4\mu m$ and $\sim 3.4\mu m$ for hole diameters respectively of $294nm$ and $268nm$ while a value larger than $4\mu m$ for the $216nm$ diameter case. Keeping in mind that the key element allowing enhanced transmission is the SP propagation over several periods of the array, it is clear that the maximum transmission of the array will reach saturation when its lateral size becomes much bigger than $l_{SP_{max}}$. Figure 2(d) presents the theoretical FWHM. As with the transmission intensities, the experimental trends are well reproduced by the simulations despite the difference in absolute values as discussed earlier. Interestingly, for low number of holes the resonance becomes sharper as d increases, the SP scattering by the holes becoming more effective. This is exactly the opposite of what happens in the large number of holes limit we discussed previously.

The above experiments show that as the hole diameter decreases for a given period, the SP propagation length increases, resulting in larger field enhancements on the surface of the array. Consequently, the transmission efficiency relative to a single hole is expected to rise when d decreases. Moreover, calculations (data not shown) indicate that the transmission efficiency of an infinite array increases with the ratio P/d.

3. Relative efficiency of the enhanced transmission

To have an idea of the relative enhancement that can be achieved, we compared the transmission of an hole array to the transmission of a single isolated hole. For this part of the study, we fabricated square arrays made up of 40×40 holes ($P = 430nm$) and their corresponding single holes, for hole diameters of $d = 150, 200, 250$ and $300nm$. Scanning electron microscope (SEM) images for the $d = 300nm$ case are rendered in Fig. 3. All the structures were milled in the same $295nm$ Au film deposited on glass substrate. An index matching liquid tuned to the refractive
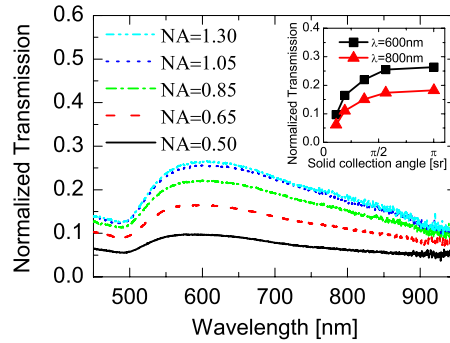
Fig. 4. (Color online) Transmission spectra of a $d = 300nm$ single hole milled in a $295nm$ thick Au film obtained by increasing the numerical aperture of the collecting objective. Each curve is an average of the spectra of 3 isolated holes of the same dimensions. Inset: Measured transmission as a function of the solid angle of collection evaluated at $600nm$ and $800nm$.

index of glass is put afterwards on top of the structure in order to work again in a symmetrical configuration. At this point it must be stressed that great care was taken during the fabrication process to achieve the same quality in milling large hole arrays and single isolated holes. The choice of the 40×40 size array was large enough for the transmission to be at saturation for four diameters considered (in the presence of index matching liquid) and still allow the fabrication of high quality hole arrays within discretization capacity of the FIB. SEM images of our structures show that geometrical parameters differ by less than $10nm$ from the specified value.

Optical characterisation of a single hole is a delicate task. Indeed a single subwavelength hole, as point source, diffracts strongly over a large spectral range, inducing geometrical aberrations. Therefore, great care must be taken in measuring single holes under a microscope to obtain the correct spectral data. Measurements were made at different focal planes to correct for the chromatic aberrations and checked against values obtained in narrow spectral windows with bandpass filters (data not shown here). A second major issue arises from the finite collecting angle of our setup. Indeed, while textbooks predict that such small apertures emit over 2π, emission pattern studies indicate that this is probably not the case for such apertures in metal films [5, 25]. Nevertheless we collected the single holes transmission with a high numerical aperture (NA) objective, namely an oil immersion objective (Nikon Plan Fluor $100\times$) with adjustable NA. We measured transmission spectrum of single hole with increasing NA (see Fig. 4. for $d = 300nm$), measured intensity increase with NA as we collect a bigger fraction of the emission pattern of the single hole and eventually reach saturation (see inset of Fig. 4.) indicating that most of the emission pattern has been collected. Saturation occurs for a collection fraction of approximately a quarter of the the half sphere, corresponding to a diffraction angle of roughly $\pm 40°$ in good agreement with previous investigations [5, 25]. Although an increase of the directivity of the diffracted field is expected as d and/or ε_m increase [26, 27], we evaluated this effect to be negligeably small within our measurement conditions.

Figures 5(a) and 5(b) show the transmission spectra of hole arrays and those of the corresponding single holes. As expected the transmission increases with hole diameter, being enhanced at some wavelengths or suppressed at other wavelengths as compared to the isolated holes. Furthermore the transmission peaks become broader with increasing hole diameter as we have already discussed before and show a slight red shift as already observed [28]. In addition transmission value at transmission minima increases with the hole diameter indicating that direct transmission through the hole array increase. Note that Fabry-Perot modes have been pre-
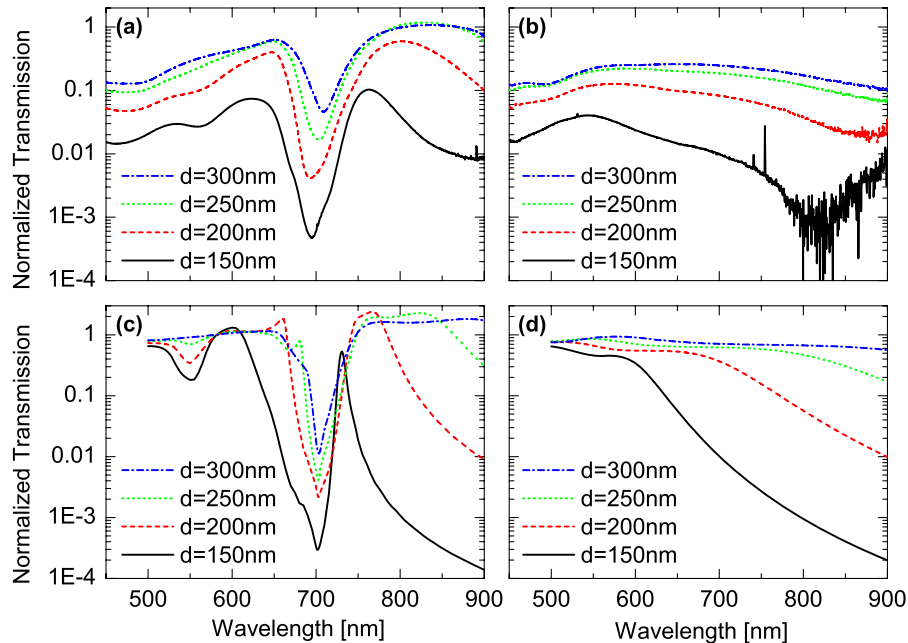
Fig. 5. (Color online) (a) and (b) Respectively experimental transmission spectra of an array of 40×40 holes ($P = 430nm$), and a single hole made in the same $295nm$ Au film with increasing diameter ($d = 150, 200, 250$ and $300nm$). The film was deposited on a glass substrate and covered with an index matching fluid ($n = 1.53$). The increase of transmission and of the noise in the long wavelength limit mainly visible for the $d = 150nm$ hole correspond to the noise level of our experimental setup which typically increase with the wavelength. For all the structures, the transmitted light as been collected using the same objective (Nikon Plan Fluor $100\times$) with numerical aperture fixed to 1.3. Each single hole curve is an average of the spectra of 3 isolated holes of the same dimensions. (c) and (d) Corresponding theoretical results. All the data are presented in logarithmic scale.

dicted to give a strong spectral signature when the holes are filled with a high index dielectric [29]. In the index matching conditions used here, calculations (not shown) indicate that such Fabry-Perot modes are very weak and broad which explains why their spectral signature is not apparent.

The ratio of the transmission of the array to that of the single hole over the whole spectral window is shown in Fig. 6(a). This representation permits us to easily follow the enhancement factor of an array relative to a single isolated hole. At the main resonance this enhancement is approximately 8, 12, 18 and 40 for $d = 300, 250, 200$ and $150nm$ respectively. The resonance at smaller wavelength corresponding to the $(1,1)$ mode display much smaller enhancement due to the fact that Au becomes increasingly unfavourable to SPs as the wavelength decreases [30]. Below ca. $500nm$, SPs cannot be sustained due to the value of the real part of the Au dielectric constant [30]. Theoretical results are rendered in Figs. 5(c), 5(d) and 6(b) showing a good qualitative agreement with the experimental findings. In these calculations we have assumed that the holes are also filled with a dielectric of refraction index equal to 1.53.

It is interesting to note that outside of the SP resonances of the hole arrays, the transmission ratios are roughly unity and essentially independent of hole diameter. On the other hand, the enhancement factor at resonance does increase as the diameter decreases, since the SP propagates further, as discussed earlier. This confirms yet again the importance of SPs in enhancing
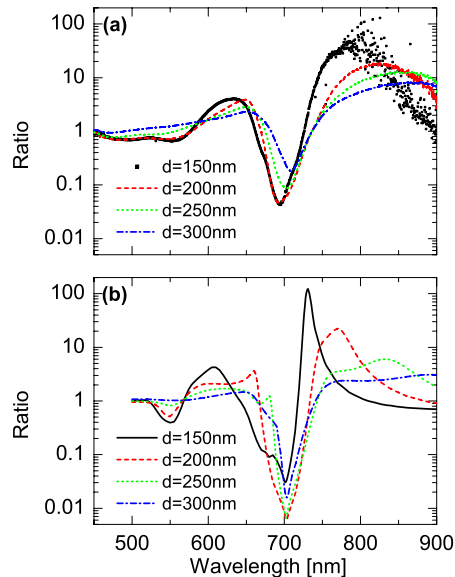
Fig. 6. (Color online) (a) Ratio of the transmission of the array to the transmission of the corresponding single hole for $d = 150, 200, 250$ and $300nm$. (b) Corresponding theoretical results. All the data are presented in logarithmic scale.

the transmission of hole arrays.

4. Conclusion

When compared to early theoretical predictions such as the work of Bethe [31], the EOT phenomenon gives rise to orders of magnitude more transmission through subwavelength apertures. However, such studies did not consider transmission resonance observed experimentally for single hole in optically thick metal films [5]. Such resonance features are also reproduced in recent numerical simulations [7-11]. The presence of a resonance in the single hole transmission spectra can already enhanced the transmission at selected wavelengths making array enhancement also dependent on the hole shape [4-6]. The transmission enhancement of an array relative to a single hole is therefore totally dependent on geometrical factors and as a consequence it is also wavelength dependent [30]. Nevertheless, the presence of well-defined SP resonances related to the periodicity of the array further enhances the transmission by one to two orders of magnitude as shown here. The best enhancement are obtained when the array is larger than the SP propagation length and the relative enhancement increases as hole diameter decreases. Although in the practical implementation, materials and fabrication issues will limit the maximum enhancement that can be reached, it is important to note that there is no theoretical fundamental upper limit to the possible enhancement attainable in the EOT process.